Influence of Vection-Induced Images on Autonomic Regulation Evaluated by Time-Varying Behavior of Motion Vectors

Tohru Kiryu[1], Yoko Nanbo[1], Eri Nomura[1], Michihiro Kobayashi[1], Naoki Kobayasi[2], and Takehiko Bando[3]

[1]Graduate School of Science and Technology, Niigata University, Niigata, Japan
[2]NTT Cyber Space Laboratories, Yokosuka, Japan
[3]Graduate School of Medical and Dental Sciences, Niigata University, Niigata, Japan

***Abstract*—Virtual reality (VR) is promising technology, but at the same enlarges another problem called cybersickness. Aiming at suppression of cybersicknes, we are investigating the influences of vection-induced images on autonomic regulations quantitatively. Using estimated motion vectors, we further synthesized random-dot pattern images as contents-free images. In a test by synthesized images, we surveyed which component of the global motion vector seriously affected the autonomic regulation. The results showed that the zoom component would induce sickness and under unpleasant situation the time-frequency representation of motion vectors revealed the switching behavior of a dominant vibration frequency that was related to camera work. We finally demonstrated the system function approach by the multivariable ARX model and successfully correlated the global motion vectors and the low-frequency power of blood pressure. As a result, the system function approach will benefit to predict the levels of cybersickness for individuals.**

***Keywords*—cybersickness, autonomic regulation, motion vector, vection, multivariable ARX model**

I. Introduction

Development of digital imaging technology by computer graphics is producing many image formats, resolutions, frame rates, in addition to conventional factors such as screen sizes, brightness, colors, and display devises. Moreover, it expands broadcasting channels including the Internet. Besides, it is most important that we can easily use brand-new digital imaging technology as movie applications in PCs and handy video cameras. Contrary to the benefits, digital imaging technology is widely spreading unexpected visual stimulus. First of all, handy cameras produce unexpected vection-induced images at ease and audience sometimes feel unpleasant for such off-centering images. Harding [1] analyzed video image factors that evoked photosensitive seizures, and produced a screening instrument for broadcasting video images. He pointed out that flashing and some specific patterns cause bad influences on brain. Not only entertainment, but also practical problems are emerging especially in the virtual reality (VR) or the virtual environment (VE). The VR is a promising technology to expand our sensory and physical functions toward outside. However, some problems have emerged recently in relation to visual stimulus. Stanney *et al.* [2] reviewed human factors issues in VEs in 1999. In 2002, Nichols *et al.* [3] has pointed out health and safety implications of VR to make recommendations regarding the future direction of VR. Hence, vection-induced problems have enlarged in practical applications of VR. Regarding visually induced motion illusions, it has been reported that the mismatch between visual system and vestibular system for vection-induced images causes sickness (sensory conflict theory) [4]. However, details in relation to sickness have been still unknown and knowledge on the visual factors that would significantly cause cybersickness or motion sickness is now wanting.

Cybersickness is unpleasant situation under VE. Unpleasant situation could be assessed by autonomic nervous activity related indices estimated from biosignals. Relatively few researchers, however, have examined vestibular-autonomic interaction in humans. Only the exposure time of visual stimuli was considered to study for optokinetic stimulation [5]. Actually, the sensory activities work with several tens of milliseconds, whereas the autonomic regulations need several seconds. Thus, there is a large difference in time-scale between autonomic activity and sensory systems (Fig. 1). This might be a reason why there are small numbers of researchers in this trans-disciplinary field.

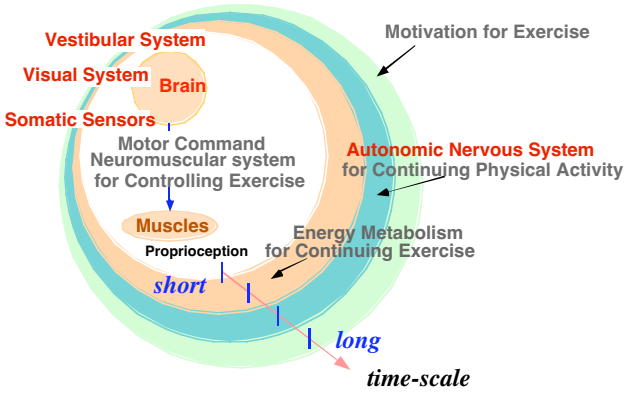

Fig. 1. Several time-scales in biosignals.

In this paper, we measured electrocardiogram (ECG), blood pressure, and respiration, while viewing vection-induced image video. Since we cannot measure visual stimulus directly, we quantized vection-induced images by motion vectors that are used in image data compression as a key technology [6]. As a similar parameter, So *et al.* tried to propose a metric for quantifying virtual scene movement by the spatial velocity [7]. The motion vector has superiority in terms of wide applicability for all of images and also convenience for surveying digital images transmitted via the Internet. Since biosignals and motion vectors were available as a function of time, we analyzed them by the time-frequency representations, and estimated the relationship between the autonomic responses and the image components while watching vection-induced images. As a new feasibility approach, we synthesized a random-dot pattern whose motion vectors are the same as those of the vection-induced real image. By changing the combination of motion vectors in synthesized images, we tried to identify which components of motion vectors were significantly related to the cybersickness.

II. Methodology

A. Experimental Procedure

Healthy young eight male and two female subjects (22.5 ± 1.5 yrs. old) participated in the experiments [8]. The subjects were informed of the risks involved in advance, and their ECG, blood pressure, and respiration were monitored at the posture of sitting down in the chair during the experiments. The ECG was measured on the chest and the continuous blood pressure was measured by a tonometry method (JENTOW7700, Colin). The respiration was measured with sensors around the chest and the abdomen (TR-755T, Nihon-Kohden). These biosignals were sampled at the rate of 1,000 Hz with a 16-bit resolution. The image was back-projected on an 80-inch screen by the video projector (TH-L795J, Panasonic) with XGA and 1,400 ANSI lumen. The distance between a subject and the screen was 2-meters and the illumination was 10 lux.

For the 18-min length visual tasks, eleven sessions of different sports experiencing images with vection were used. In particular, we selected the image of mountain bike riding because almost all the subjects felt unpleasant conditions while and after watching the video image. Note that the video camera attached at the top of the mountain bike handle produced unexpected camera work. Furthermore, we synthesized a random-dot pattern image by CG whose motion vectors were the same as those in the mountain bike riding image. By the sequential epoch method [9], we tried to identify which component is related to the cybersickness. Based on the sequential epoch method, each experimental set consisted of consecutive six trials with a sequence comprised 2-minute exposure followed by 1-minute rest. Note the there was 3-minutes rest and 3-minutes exposure of random-dot still picture ahead of the consecutive six trials.

B. Motion Vector

We estimated the motion vectors in each section of a screen for the image size of 352×288 pixels by the block matching method [6]. Note that the whole image was divided into 25 (5×5) sections. Moreover, the motion vector was estimated in the block of 8×8 pixels and then averaged in each section to estimate the averaged local motion vector (LMV). Besides, a global motion vector (GMV), which is similar to the motion of camera, was estimated from LMV by a bottom-up approach [10].

We synthesized random dot CG images by a graphic system (VSG2/5, Cambridge Research Systems) referring to the GMV estimated from the real mountain bike riding image. We studied the effects of GMV with respect to zoom, pan, and tilt components, separately. Note that there were five experimental sets for differences between GMV and LMV, among GMV components, among LMV components, among vibration frequency bands of GMV (0–1 Hz, 0–2 Hz, 0–4 Hz, and 0–8 Hz), and among vibration frequencies of GMV for switching behavior (switching between 0–1 Hz and 0–8 Hz, 0–2 Hz and 0–8 Hz, and 0–4 Hz and 0–8 Hz).

C. Signal processing

We studied autonomic nervous activity (ANA) by calculating the power at limited frequency ranges of blood pressure and respiration. We used the wavelet transform (WT) to estimate the time-varying behavior of powers in the limited frequency ranges by the Gabor function as a mother wavelet.

The sampling rate of biosignals was adjusted to the frame rate of images. Since the frame rate was 30 frames/sec, we uniformly resampled R-R interval from ECG at the frequency of 30 Hz. Blood pressure and respiration were also resampled at 30 Hz. In extraction of ANA related indices, the limited frequency rages are 0.04–0.15 Hz for blood pressure and R-R interval (Mayer wave related signal), and 0.16–0.45 Hz for respiration and R-R interval (respiratory sinus arrhythmia related signal) [11]. Then, we obtained the time-series of the ANA related indices every frame with a 10-sec interval and the averaged motion vectors in each sliding window with a 10 sec interval. The sliding window was shifted every frame.

Furthermore, to compare the ANA related indices among subjects, we normalized each ANA related power by the averaged power during resting phase ahead of each experiment. For evaluating the effect of GMV components by synthesized random-dot pattern images, we estimated a variation ratio that is an ANA related

index under the scene with full GMV components divided by that without a specific GMV component. Accordingly, the ANA indices were the normalized low-frequency (LF) power of blood pressure, the normalized high-frequency (HF) power of respiration, the normalized LF and HF powers of R-R interval, and those variation ratios. Note that the time-varying behavior of motion vectors were also analyzed by the WT with the same conditions of biosignals.

Sensory stimulus possibly disturb the autonomic regulations. Evaluating the autonomic regulations under sensory disturbance, we estimated the system function by the multivariable ARX model (AR refers to the autoregressive part and X to the extra input [12]) for sensory stimuli as the input and ANA related indices as the output (**Fig. 2**). The ARX model is given by.

$$y(t) = \sum_{i=1}^{n_a} \alpha_i y(t-i) + \sum_{j=1}^{n_b} \beta_j u(t-j-n_d) + e(t)$$

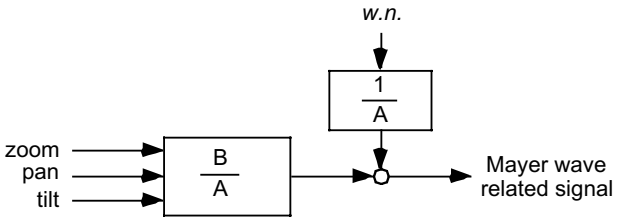

Fig. 2. System function approach for virtual motion.

III. Results

Figure 3 demonstrates the time-series of the pan component of GMV and its time-frequency representations by the WT.

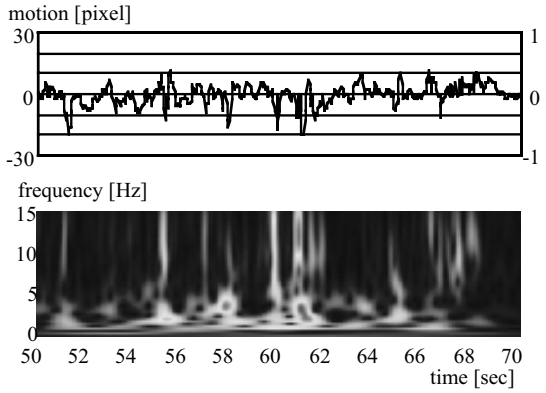

Fig. 3. Pan component of GMV and its Wavelet transform.

Regarding the variation, the mountain bike riding image included switching behavior of dominant vibration frequency; that is, the dominant vibration frequency varied between around 2 and 5 Hz in the 50–70 interval. Note that the exposure times of high and low vibration frequencies were about 2.0–3.0 sec. Thus the vection-induced real images were characterized by the time-varying behavior of motion vectors and appearance of camera work at each section.Five subjects felt unpleasant for the mountain bike riding, bobsleigh, and bike race sessions. Autonomic response of each subject while watching the mountain bike riding image and the synthesized random-dot pattern image was featured by the normalized low frequency power of blood pressure and the normalized high frequency power of respiration in **Fig. 4**. Unpleasant state occurred in random dot pattern for Fig. 4(a), whereas it happened in real image for Fig. 4(b). As a result, the normalized low-frequency power of blood pressure increased and the normalized high-frequency power of respiration fluctuated under unpleasant situation, regardless of the real and the synthesized random-dot pattern images. Referring to experiments by random dot pattern images, most significant components of GMV were zoom and pan (Fig. 5) by removing or adding the components in synthesized images.

After evaluating the time-varying features of GMV and the ANA related indices, we estimated the system function by the multivariable ARX model. From the first half of the mountain bike riding image in **Fig. 6(a)**, we estimated the parameters of the multivariable ARX model for data consisted of the LF power of blood pressure and the GMV components: zoom, pan, and tilt. The length of interval for estimation was 50 sec. The appropriate n_d was 90 under the condition that n_a and n_b, were 2. The results showed that the multivariable ARX model allowed us to predict the LF power of blood pressure at the latter half of the mountain bike riding image. Then, we applied these parameters to other image, a bike race image. The results demonstrated that the LF power of blood pressure was successfully estimated by the parameters that were determined at the first half of the mountain bike riding image (Fig. 6(b)). Note that the time-delay was depended on each individual and the multivariable ARX model showed best fit for the LF power of blood pressure as the output.

IV. Discussion

The influences of vection-induced images were caused by many different factors. One of the factors is the video contents which link to the experience of each subject. Another factor is related to camera work. When camera work is hard to be purchased, subjects feel unpleasant situation. That is, vection-induced images with a certain exposure time interval could enlarge the sensory conflict [4] and in turn disturb the autonomic regulations [13]. The evidence for real images is,

however, difficult to assess because visual stimuli is hard to evaluate quantitatively.

We investigated the motion vector that is rather a contents-free factor and represent the camera work. The time-frequency representation of motion vectors demonstrated the switching behavior of dominant vibration frequency in the mountain bike riding image. Since half of the subjects felt unpleasant situation for the mountain bike riding image, the expected reasons for cybersickness would be switching the vibration frequencies in motion vectors. The low vibration frequency ranged from 0.5 to 2 Hz. Actually, it was also reported that a motion sickness enlarges around the 0.2 Hz frequency range of horizontal translational oscillation [19]. Although the motion vectors alone do not present all of the features, the time-frequency representation allowed us to preset the candidates that possibly disturb autonomic regulations.

Conventional studies have not reported the influences of vection-induced images by the input-output relationship quantitatively. One of the reasons is the time-delay between input stimulus and output responses. Due to the time-delay the exposure time and the intensity of visual stimuli might be related to the autonomic regulations afterward. Using GMV components and the LF power of blood pressure, we expected 1–10 sec as the time delay for visual stimuli for autonomic response in the multivariable ARX model. Since the time-delay was depended on each individual and the LF power of blood pressure was best fit as the output, the multivariable ARX model would allow us to feature the individual characteristics for the vection-induced images.

In our experiments, however, the autonomic regulations were not so clearly different between real and virtual movement (Fig. 4). Something happened, but there were not consistent. Only the restricted images, the synthesized random-dot pattern images, showed some meaningful tendency. Since such the mismatch under unexpected vection-induced images is not set up in the brain in advance, the levels of sickness could be related to robustness of autonomic regulation for individuals.

V. Conclusion

Preventing cybersickness becomes a key point to apply virtual reality for a long time use. Cybersickness is related to factors in both images and conditions of users. We studied influences of vection-induced images in the relationships between autonomic nervous activity related indices and motion vectors of images. Autonomic nervous activity was evaluated from R-R interval, blood pressure, and respiration. The motion vectors including global and local motion vectors were estimated by the data compression technique.

According to the time-varying behavior of motion vectors, the switching behavior in the vibration frequency and, zoom and pan components of global motion vectors possibly caused cybersickness. Moreover, the multivariable ARX model as the system function approach would be effective for screening the level of cybersickness for individuals. However, we have not yet concluded whether the unpleasant feeling was caused by the content of the vection-induced image or the structure of the image scene (the frame rate, the vibration of objects, etc). Further studies are required to clarify the levels of sensory activity on autonomic regulations to block motion cybersickness.

References

[1] G. F. A. Harding, “TV can be bad for your health,” *Nature Medicine*, vol. 4, 3, pp. 265-267, 1998.

[2] K. M. Stanney, R. S. Kennedy, J. M. Drexler, and D. L. Harm, "Motion sickness and proprioceptive aftereffects following virtual environment exposure," Appl Ergon, vol. 30, pp. 27-38., 1999.

[3] S. Nichols and H. Patel, "Health and safety implications of virtual reality: a review of empirical evidence, " *Appl Ergon*, 33, 3, pp. 251-271, 2002.

[4] L. J. Hettinger, K. S. Berbaum, R. S. Kennedy, W. P. Dunlap, and M. D. Nolan, "Vection and simulator sickness," Mil Psychol, vol. 2, pp. 171-81., 1990.

[5] N. A. Webb and M. J. Griffin, "Optokinetic stimuli: motion sickness, visual acuity, and eye movements," *Aviat. Space Environ. Med*., vol. 73, pp. 351-8., 2002.

[6] K. R. Rao and J. J. Hwang, *Techniques and standards for Image, video, and audio coding*, prentice Hall, 1996.

[7] R. H. So, A. Ho, and W. T. Lo, "A metric to quantify virtual scene movement for the study of cybersickness: Definition, implementation, and verification," Presence, 10, 2, pp. 192-215, 2001

[8] T. Kiryu, Y. Nanbo, N. Kobayasi, and T. Bando, "Relationship between Motion Vectors of Vection-Induced Image and Multivariate Biosignals under Visual Tasks," in *Proc. 4th International Workshop on Biosignal Interpretation*, pp. 517-520, Como, Italy, 2002.

[9] T. Nagada, Y. Fujii, K Suzuki, I L. Kwee, "High-field (3.0 T) functional MRI sequential epoch analysis: an example for motion control analysis," Neurosci. Res., Vol. 32, No. 4, pp. 355-362, 1998.

[10] K. Jinzenji, H. Watanabe, and N. Kobayashi, Global motion estimation for static sprite production and its application to video coding, IEEE ISPAC’98, pp. 328-332, 1998.

[11] S. Akselrod, D. Gordon, F. A. Ubel, D. C. Shannon, A. C. Berger, and R. J. Cohen, "Power spectrum analysis of heart rate fluctuation: a quantitative probe of beat-to-beat cardiovascular control," *Science*, vol. 213, pp. 220-222, 1981.

[12] L. Ljung, *System identification: Theory for the user*, Englewood Cliffs: PTR Prentice Hall, 1987, ch. 4.2

[13] J. F. Golding, M. I. Finch, and J. R. Stott, "Frequency effect of 0.35-1.0 Hz horizontal translational oscillation on motion sickness and the somatogravic illusion," *Aviat. Space Environ. Med*., vol. 68, pp. 396-402., 1997.

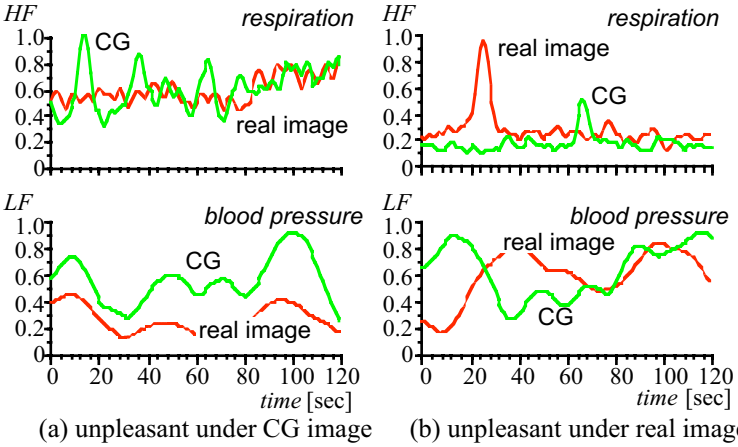

Fig. 4. HF and LF normalized power for real image and random dot pattern image: (a) Unpleasant state occurred in random dot pattern; (b) whereas it happened in real image.

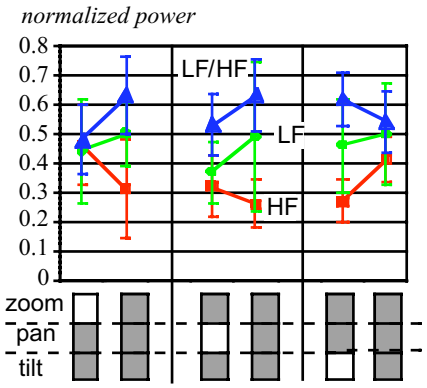

Fig. 5. Influence of the components of motion vector. Adding zoom and pan enlarged LF and LF/HF.

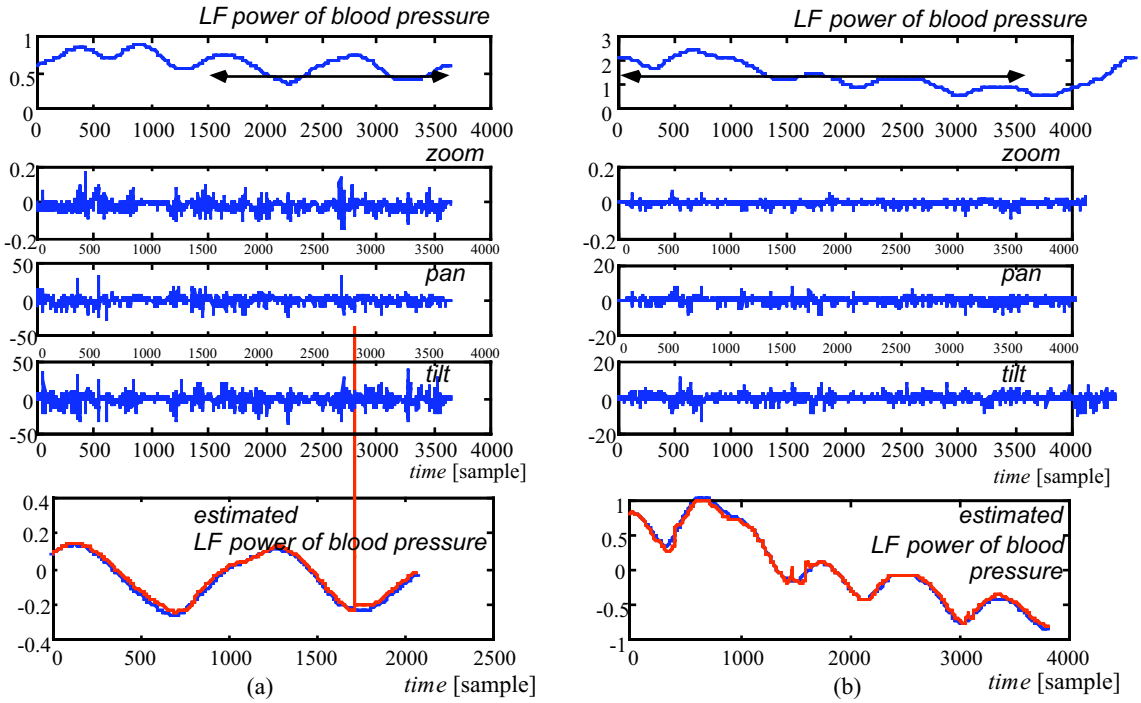

Figure 6. Results by the multivariable ARX model for (a) mountain bike riding scenes and (b) bike race scenes. From top to bottom, the LF power of blood pressure as an output, the global motion vectors as inputs, and the estimated LF power of blood pressure. Arrows show intervals for estimating the multivariable ARX model parameters.